https://doi.org/10.55343/CogSust.20525

Microturbine design for sustainable fuels

Peter Kondor
John von Neumann University
Kecskemet, Hungary
kondor.peter@nje.hu

Abstract
The global shift toward sustainability and the urgent need to reduce reliance on fossil fuels have intensified research into alternative energy carriers across transportation and power generation sectors. Gas turbines and microturbines, known for their high efficiency and operational flexibility, offer a promising platform for integrating low-carbon fuels into electricity production. This study presents the design of an experimental microturbine developed to examine the combustion characteristics of sustainable gaseous fuels – specifically hydrogen and biogas – under controlled laboratory conditions. The investigation focuses on fuel applicability, combustion stability, and emission profiles, contributing to developing cleaner and more sustainable energy conversion systems. The microturbine is constructed using a commercially available automotive turbocharger, featuring a centrifugal compressor and a centripetal turbine, paired with a custom-designed counterflow combustion chamber. Component selection and chamber design are guided by engineering calculations and a thorough literature review, ensuring mechanical compatibility and experimental reliability. The setup provides a scalable and accessible platform for advancing sustainable combustion technologies.

Keywords
microturbine, sustainable fuel, emission, energetics

1. Introduction

Thanks to their unique blend of efficiency, flexibility, and environmental benefits, microturbines play a crucial role in modern energy production. Microturbines are ideal for decentralised power systems, allowing energy to be produced close to where it is consumed. This reduces transmission losses and enhances grid resilience. They efficiently generate both electricity and usable heat from a single fuel source. This dual output makes them perfect for industrial facilities, commercial buildings, and residential complexes. Microturbines can run on various fuels, including natural gas, biogas, and hydrogen. This adaptability supports the transition to cleaner energy sources.

These systems produce significantly lower nitrogen oxides (NOx) and carbon monoxide (CO) levels than traditional combustion engines, helping meet strict environmental regulations. Microturbines can reach full capacity in under two minutes and adjust quickly to changing energy demands, making them excellent for backup power and peak load support. Their small footprint and low noise make them suitable for urban environments and space-constrained installations. Multiple units can be combined to meet larger energy needs, offering scalability without sacrificing efficiency.

Microturbines are increasingly important as we shift toward a carbon-free energy grid. They complement intermittent renewable sources like solar and wind by providing reliable backup and grid stability. Their ability to hybridise with renewables and operate off-grid makes them a cornerstone of sustainable energy systems.

2. Background: Thermodynamics of the operating principle of gas turbines

The air-standard Brayton cycle is ideal for the simple gas turbine (GT). The simple open-cycle GT utilises an internal-combustion process, and the simple closed-cycle gas turbine utilises heat transfer (Mikielewitz et al, 2019a). Both cycles are schematically shown in Figure 1.

https://doi.org/10.55343/CogSust.20525

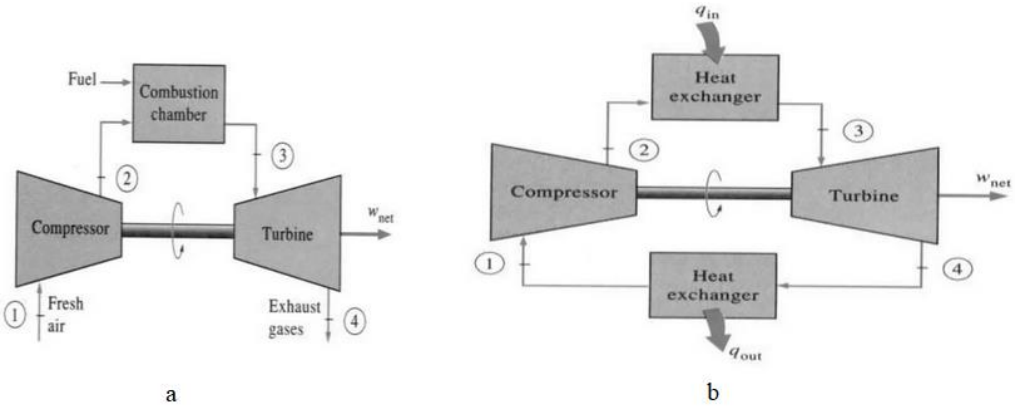

Figure 1. Gas turbine cycles (a) Open-cycle, (b) Closed-cycle

The thermal efficiency (η_t) of a simple Brayton-cycle can be determined based on the following Equation (1), based on (Korakianitis, Wilson, 1994):

$$\eta_t = 1 - \frac{T_4 - T_1}{T_3 - T_2} = 1 - \frac{1}{\left(\frac{p_2}{p_1}\right)^{\frac{K-1}{K}}} = 1 - \frac{1}{(\pi_k)^{\frac{K-1}{K}}} \quad (1)$$

It depends on the pressure ratio (π) of the compressor and the specific heat ratio of the working fluid *(K)*.

The total output work *(W)* is derived from the difference between turbine work *(W_t)* and compressor work *(W_c)*, equation (2).

$$W = W_t - W_c \quad (2)$$

The efficiency increase with pressure ratio is evident from the entropy diagram of the simple Brayton cycle, as shown in Figure 2.

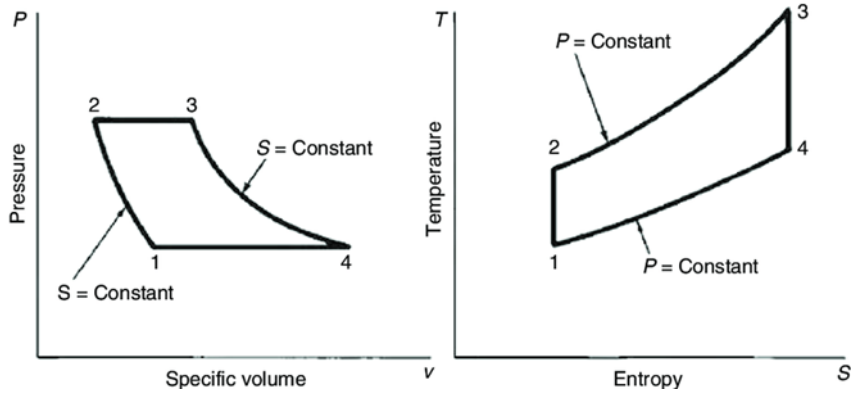

Figure 2. P-V and T-S diagrams of a standard air Brayton-cycle

The fuel required to raise the temperature from 2 to 3 is:

$$\dot{m}_f = \frac{h_3 - h_2}{LHV\eta}\,[\text{kg}] \quad (3)$$

where h_2 and h_3 are the enthalpies, the *LHV* is the lower heating value, and η is the thermal efficiency. Many fuels can be used in gas turbines (Mikielewicz et al., 2019b) because, due to their operating principle, they are

https://doi.org/10.55343/CogSust.20525

less sensitive to calorific value than piston engines. Table 1 shows the classification of applicable fuels according to their calorific value (Hunicz et al., 2020; Annamalai et al., 2016; Emőd et al., 2005; Zöldy and Kondor, 2021).

Table 1. Classification of fuels

Classification of fuel	Typical composition	LHV [MJ/kg]	Typical specific fuels
Ultra Low LHV gaseous fuels	H_2 < 10% CH_4 < 10% N_2 + CO > 40%	< 11.200 (< 300)	Blast furnace gas Inert gas Biogases
High hydrogen gaseous fuels	H_2 > 50% C_xH_y = 0–40%	5.500–11.200 (150–300)	Refinery gas Petrochemical gas Hydrogen power
Medium LHV gaseous fuels	CH_4 < 60% N_2 + CO_2 = 30–50% H_2 = 10–50%	11.200–30.000	Weak natural gas Landfill gas, Coke oven gas, Corex gas
Natural gas	CH_4 = 90% C_xH_y = 5% Inert = 5%	30.000–45.000	Natural gas Liquefied natural gas
High LHV gaseous fuels	CH_4 and higher hydrocarbons C_xH_y > 10%	32.000–45.000	Liquid petroleum gas (butane, propane) Refinery off-gas
Liquid fuels	C_xH_y, with x > 6	32.000–45.000	Kerosene, Diesel oil, Naptha, Crude oils, Residual oils, Bio-liquids

Source: own compilation based on (Canakci, Sanli, 2008), (Suchockiet al., 2023).

3. Combustion chamber selection for experimental application

A counterflow combustion chamber is a special design commonly used in gas turbines and microturbines, where the hot combustion gases flow opposite to the incoming compressed air. This reversed, U-shaped flow path makes the chamber more compact and reduces the overall engine length compared to straight-through combustors. Compressed air enters at the rear section and flows forward around the combustion liner, with part of the air being directed through swirlers and holes into the liner for fuel–air mixing. Fuel is injected into the liner and stabilised by vortex generators or swirl vanes, creating a stable flame and efficient combustion. Meanwhile, cooling air flows along the outer liner walls to protect them from excessive heat, while dilution holes near the downstream section introduce additional air to reduce the exit temperature before the gases turn back toward the turbine inlet. This counterflow arrangement not only helps with compactness but also improves thermal management of the casing, as the reversed gas flow distributes heat more evenly. Efficient mixing of fuel and air is critical to avoid hot spots and to maintain low emissions, often supported by staged fuel injection. At the same time, the design reduces pressure losses compared to long straight combustors, which increases efficiency (Casey, Schlegel, 2010). Despite these advantages, the counterflow combustor must be carefully engineered to ensure uniform temperature distribution at the turbine inlet and to withstand high thermal gradients and cyclic loads. This configuration combines compact size, effective cooling, and stable performance, making it a reliable choice in many modern turbine applications. Based on literature research, the planned combustion chamber construction is shown in Figure 3.

https://doi.org/10.55343/CogSust.20525

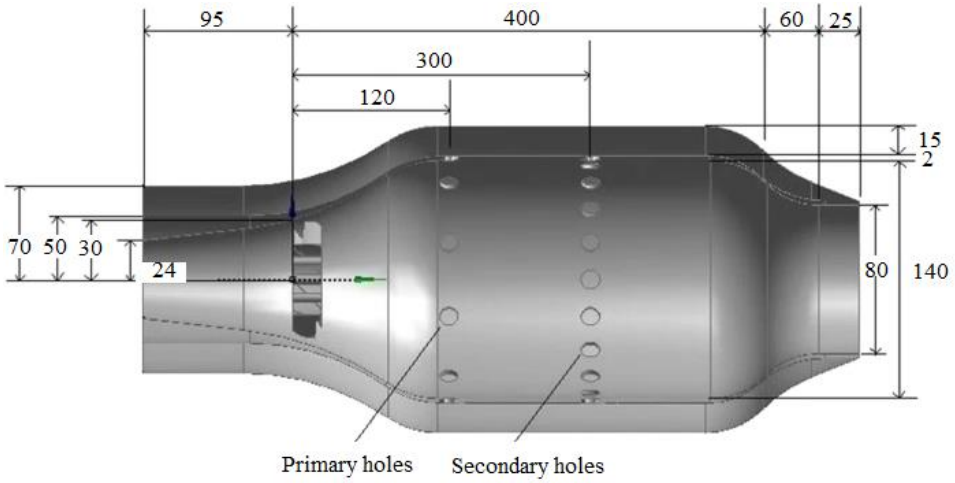

Figure 3. Designed counterflow combustion chamber dimensions

The combustion chamber is made of a 2 mm thick stainless KO36Ti plate. When designing the combustion chamber, flow simulations were performed based on the mass flow of the centrifugal compressor, during which the development of the velocity conditions in the primary and secondary zones and the temperature distribution in the combustion chamber segments had to be examined. The velocity vectors and temperature distribution based on simulations are shown in Figure 4.

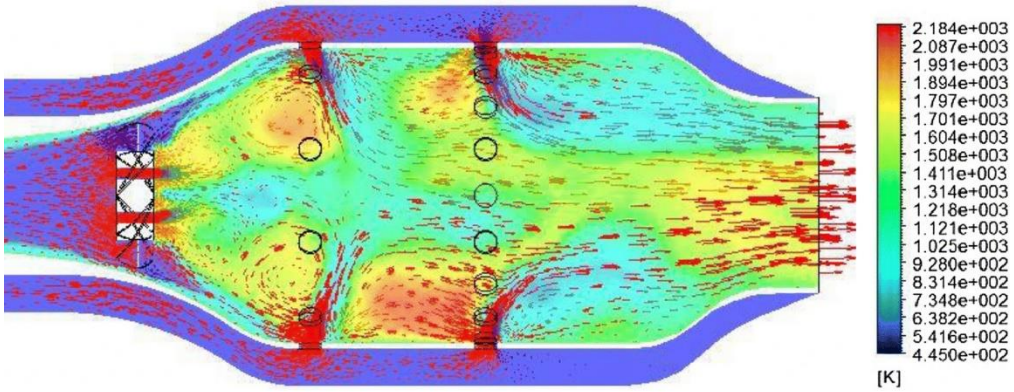

Figure 4. Velocity vectors and temperature distribution based on simulations

4. Compressor and turbine selection

A Garrett G40-1150 turbocharger powers the microturbine compressor and turbine unit. The data required for sizing is provided by the measured characteristic of the centrifugal compressor, which is shown in Figure 5.

https://doi.org/10.55343/CogSust.20525

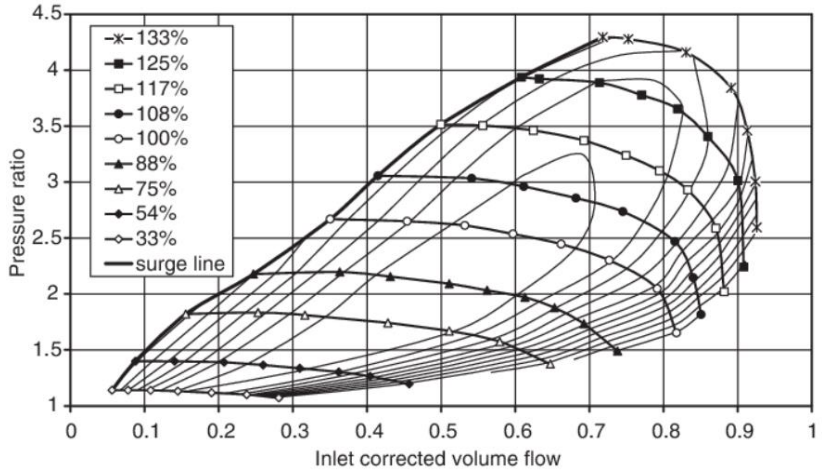

Figure 5. Compressor characteristic for the turbocharger centrifugal compressor

The pressure ratio can be determined based on the best efficiency curve as a value close to 3. The corresponding mass flow rate is 0.6 cubic meters per hour. The density at the inlet can be determined using Equation (3).

$$Q_0 = \frac{p_0}{R \cdot T_0} \tag{3}$$

The pressure is reduced to half the cross-section, based on simulation measurements between approximately 97000 Pa. From the pressure ratio, the combustion chamber pressure can be determined using Equation (4).

$$\pi = \frac{p_2}{p_1} \rightarrow p_2 = p_1 \cdot \pi \tag{4}$$

From the magnitude of the inlet and outlet pressures and the inlet density, the outlet density can be derived from the Bernoulli equation, which gives the density of the air entering the compressor. By writing and rearranging the Poisson equation (5), the outlet temperature of the confuser can be calculated.

$$\frac{T_1}{T_0} = \left(\frac{p_1}{p_0}\right)^{\frac{K-1}{K}} \rightarrow T_1 = T_0 \frac{p_1}{p_0}^{\frac{K-1}{K}} \tag{5}$$

The compression and expansion processes show an increase in entropy of Δs due to the flow and friction losses, which were still negligible in the inlet confuser. Here, the air filter that may be placed in front of the compressor must consider the gap and friction losses on the shaft. In practice, the compressor efficiency is determined based on these losses. This loss can be ignored since there is no air filter in front of the compressor. In order to achieve a constant pressure ratio in the compressor, a greater enthalpy change is required due to the losses, which means introducing a higher compressor power, which is why more heat is generated. The compressor power requirement can be calculated based on Equation (6).

$$P_k = \dot{m} \cdot c_p \cdot (T_2 - T_1) \tag{6}$$

When designing the combustion chamber, a conventional propane-butane gas was selected. Propane (C_3H_8) and butane (C_4H_{10}) are available in different proportions, but the most commonly used mixture is 60% propane and 40% butane. The heat output can be calculated using the following Equation (7):

$$\dot{Q} = \dot{m} \cdot c_p \cdot (T_3 - T_2) \tag{7}$$

Based on this, the calculated heat output during propane-butane combustion is 350 kW. When calculating the turbine power, it must be taken into account that the turbine can process a smaller enthalpy change with an

https://doi.org/10.55343/CogSust.20525

unchanged expansion pressure ratio, which results in a smaller extractable P_t turbine power. The ideal temperature, actual temperature and actual power of the turbine can be derived from the Poisson equation. The system's total power is the difference between the power of the turbine and the compressor, since part of the energy produced by the turbine is used to work in the compressor. The efficiency can be calculated by considering the losses occurring in the compressor, the combustion chamber and the turbine. The effective power of the designed microturbine is 60 kW with propane-butane fuel.

5. Conclusion

The study presents the design of an experimental microturbine, which aims to research and test sustainable fuels, mainly based on aspects of emission and applicability. The microturbine consists of a conventional automotive turbocharger and a unique counterflow combustion chamber designed based on literature research. After the construction of the microturbine, it will be possible to test gaseous and liquid components such as hydrogen, biogas, plant-based and recycled fuels and their mixtures in laboratory conditions.

References

Annamalai, M., Dhinesh, B., Nanthagopal, K., SivaramaKrishnan, P., Lalvani, J. I. J., Parthasarathy, M., Annamalai, K. (2016). An assessment on performance, combustion and emission behavior of a diesel engine powered by ceria nanoparticle blended emulsified biofuel. *Energy Conversion and Management.* 123, 372–380. DOI: https://doi.org/10.1016/j.enconman.2016.06.062

Canakci, M., Sanli, H. (2008). Biodiesel production from various feedstocks and their effects on the fuel properties. *Journal of Industrial Microbiology and Biotechnology*. 35(5), 431–441, https://doi.org/10.1007/s10295-008-0337-6

Casey, M. V., Schlegel, M. (2010). Estimation of the performance of turbocharger compressors at extremely low pressure ratios. *Proceedings of the Institution of Mechanical Engineers, Part A: Journal of Power and Energy*. 224(2), 239–250. DOI:https://doi.org/10.1243/09576509JPE810

Emőd, I., Füle, M., Tánczos, K., Zöldy, M. (2005). A bioetanol magyarországi bevezetésének műszaki, gazdasági és környezetvédelmi feltételei. *Magyar Tudomány*. 50, 278–286. URL: https://epa.oszk.hu/00600/00691/00015/03.html

Hunicz, J., Matijošius, J., Rimkus, A., Kilikevičius, A., Kordos, P., Mikulski, M. (2020). Efficient hydrotreated vegetable oil combustion under partially premixed conditions with heavy exhaust gas recirculation. *Fuel*. 268, 117350. DOI: https://doi.org/10.1016/j.fuel.2020.117350

Korakianitis, T., Wilson, D. G. (1994). Models for predicting the performance of Brayton-cycle engines. ASME. *Journal of Engineering for Gas Turbines and Power*. 116(2), 381–388. https://doi.org/10.1115/1.2906831

Mikielewicz, D., Kosowski, K., Tucki, K., Piwowarski, M., Stępień, R., Orynycz, O., Włodarski, W. (2019a). Gas turbine cycle with external combustion chamber for prosumer and distributed energy systems. *Energies*. 12(18), 3501. DOI: https://doi.org/10.3390/en12183501

Mikielewicz, D., Kosowski, K., Tucki, K., Piwowarski, M., Stępień, R., Orynycz, O., Włodarski, W. (2019b). Influence of different biofuels on the efficiency of gas turbine cycles for prosumer and distributed energy power plants. *Energies*. 12(16), 3173. DOI: https://doi.org/10.3390/en12163173

Suchocki, T. Kazimierski, P. Lampart, P., Januszewicz, K., Białecki, T., Gawron, B., Janicka, A. (2023). A comparative study of pentanol (C5 alcohol) and kerosene blends in terms of gas turbine engine performance and exhaust gas emission. *Fuel*. 334(2), 126741. DOI: https://doi.org/10.1016/j.fuel.2022.126741

Zöldy, M., Kondor, I. P. (2021). Simulation and injector bench test validation of different nozzle hole effect on pyrolysis oil-diesel oil mixtures. *Energies*. 14(9), 2396. DOI: https://doi.org/10.3390/en14092396